Preparation and Characterization of Nylon-6/PPy/MMT Composite of Nanocomposite

S. Jamal Peighambardoust,[1,2] Behzad Pourabbas[1,2]

[1]*Nanostructured Materials Research Center, Sahand University of Technology, Tabriz 51335-1996, Iran*
[2]*Polymeric Materials Research Center, Sahand University of Technology, Tabriz 51335-1996, Iran*

ABSTRACT: Series of composites consisting of polypyrrole/montmorillonite nanocomposites in the matrix of Nylon6 has been synthesized and characterized in this work. The composites were processable, so that test samples were prepared by compression-molding of the materials for electrical property measurements. Intercalated structures were confirmed by wide-angle X-ray diffraction and TEM studies for PPy/MMT nanocomposites. A two-phase structure was determined for the fused samples consisting of two separated N6 and PPy phases by using scanning electron microscopy analyses. A conductivity threshold was measured at 15%(w/w) loading level of PPy in the composites. Electrical resistivity–temperature behavior of the samples was investigated and a resistivity peak was observed at 100°C for the samples. It was proved that the glass transition temperature of PPy around 100°C should be the responsible factor for the observed resistivity peak, as studied by thermogravimetic analysis and differential scanning calorimetry thermal methods. © 2007 Wiley Periodicals, Inc. J Appl Polym Sci 106: 697–705, 2007

Key words: polypyrrole; Nylon-6; nanocomposite

INTRODUCTION

Substantially conducting polymeric materials have been one of the interesting research fields during recent years because of their wide range of applications such as solid state devices and electronics. However, the lack of suitable mechanical and physical properties, such as low solubility, brittleness, and low level processability, is one of the major drawbacks for such compounds.[1] Therefore, wide range of researches has been focused on resolving the problem with the conducting polymers. One way is to combine them with other polymers to produce composites and blends so that several types of conducting polymer blends and composites have been prepared and investigated for this purpose. Polypyrrole (PPy) has been one of the most studied conductive polymers because of its physical and electrical properties and also its ease of synthesis. For example, composites of PPy and ethylene vinyl alcohol,[1] polypropylene,[2] polyethylene,[3] and ultrahigh-molecular-weight polyethylene,[4,5] polyurethane,[6] polymethyl methacrylate,[7] or even with natural rubber[8] have been prepared by insertion of the conducting polymer into the polymer matrix. In such composites or blends, the conducting polymer satisfies the conductivity requirements, while the polymer matrix play the responsibility for enhanced mechanical properties in the composite.

Since 1997, after the report from the Toyota research group of a Nylon6 (N6)/montmorillonite (MMT) nanocomposite,[9] for which very small amounts of layered silicate loadings resulted in pronounced improvements of thermal and mechanical properties, polymer/clay or polymer/layered silicate nanocomposites have attracted great interest, both in industry and in academia. They often exhibit remarkable improvement in material properties when compared with virgin polymer or conventional micro and macrocomposites. These improvements can include high moduli, increased strength and heat resistance, decreased gas permeability and flammability, and increased biodegradability of biodegradable polymers.[10] Conducting polymer/clay nanocomposites were also prepared to associate the advantages of conductivity and superior properties of the polymer/clay nanocomposites. In this way, PPy/MMT nanocomposites have been prepared by several methods, including intercalation in polymer latex,[11] by emulsion[12] or inverted emulsion polymerization,[13] by electropolymerization,[14,15] and by solvent-free mechanical route.[16] Although, improved properties, for example, enhanced corrosion protection property,[17] and improved mechanical and thermal properties[13] have been reported for PPy/MMT nanocomposites, however, the major drawback of insolubility and inprocessability still remained with the nanocomposites. Preparation of a ternary composite consisting of a ther-

Correspondence to: B. Pourabbas (pourabas@sut.ac.ir).

moplastic polymer (polypropylene), PPy, and MMT was an effort toward a conductive processable composite of nanocomposite.[18,19] Different process conditions were inspected and the influence of MMT has been shown to enhance the electrical conductivity of the ternary system when compared with PP/PPy binary composites.

Preparation and characterization of ternary composites consisting of N6, PPy, and MMT has been the target of the present work. Therefore, a series of N6/PPy/MMT composites were prepared by different amounts of PPy loading in a constant level of MMT for comparative purposes. Wide-angle X-ray diffraction (WAXD), scanning electron microscopy (SEM), thermogravimetic analysis (TGA), and differential scanning calorimetry (DSC) were used as characterization tools. The electrical conductivity of the ternary composites was investigated using specific test samples prepared as sandwiched construction, by compression-molding of the test compounds between two nickel foil electrodes.

EXPERIMENTAL

Materials

Nylon 6 was Akulon[TM] F223-D (Netherlands) and used after cryogenic grinding of the granules into particle sizes less than 50 μm. Pyrrole monomer (Merck, Germany) was purified by distillation under reduced pressure before use. The oxidizing agent, ferric sulfate [$Fe_2(SO_4)_3$], was purchased from Merck, and sodium dodecylbenzenesulfonate (DBSNa) from Fluka chemical companies. The layered silicate in the present work was montmorillonite (MMT) supplied from Aldrich. All the other ordinary chemicals used in this work were laboratory-grade, mainly obtained by Merck or Fluka (Switzerland) chemical companies.

Preparation of N6/PPy/MMT composite of nanocomposite

N6/PPy/MMT composites were prepared by emulsion polymerization of pyrrole in the presence of DBSNa as the surfactant in water suspension of MMT.

A suspension of MMT was prepared by addition of appropriate amount of MMT to 150 mL distilled water and treated with a high-speed homogenizer for 1 h to obtain better exfoliation of clays. Another mixture containing N6 fine powder, which was obtained by cryogenic grinding of N6 granules, DBSNa, and pyrrole monomer in 50 mL distilled water, was prepared separately and then added into the clay suspension under vigorous mechanical stirring. After 15 min, the polymerization was started dropwise by addition of 100 mL oxidant $Fe_2(SO_4)_3$ aqueous solution. The polymerization was carried out for 4 h at room temperature under moderate mechanical stirring condition. Table I provides the amounts of materials used for preparation of N6/PPy/MMT composites with different PPy content. MMT loading in all the nanocomposites was constant at 5% by weight with respect to total weights of N6 and PPy. Constant oxidant/monomer and surfactant/monomer molar ratio was used, 1.2 and 5, respectively, for the synthesis of the composites in Table I. At the end of procedure, a black product was collected on a filter paper, washed several times with water, and then dried at 60°C for 24 h under reduced pressure.

Preparation of the reference materials

In addition to the ternary composite of nanocomposites mentioned earlier, three other compounds were prepared as the reference materials for comparison. These were PPy/MMT nanocomposites, pure PPy, and samples containing N6 and PPy only. In preparation of PPy/MMT nanocomposites, pyrrole (0.15 mol) was added to a 150 mL suspension solution of MMT (1.75 g) in distilled water. After 1 h stirring by using the high-speed mechanical homogenizer, mixture of surfactant (DBSNa, 0.03 mol) and oxidizing agent [$Fe_2(SO_4)_3$, 0.18 mol] dissolved in 100 mL distilled water was added to start polymerization. Polymerization reaction was continued for 4 h at room temperature. The products in the form of black powder were collected over a filter paper, washed several times with distilled water, and then vacuum-dried at 60°C for 24 h.[20]

Pure PPy samples were prepared by the same method without using neither N6 powder nor MMT for comparative purposes. In addition, samples con-

TABLE I
Quantity of Materials Used for the Synthesis of Compounds in This Work

Sample	Moles of monomer	Moles of $Fe_2(SO_4)_3$	Moles of DBSNa	Grams of MMT	Grams of N6
PPy	0.015	0.018	0.003	–	–
PPy/MMT	0.15	0.18	0.03	1.75	–
N6/PPy5%/MMT	0.015	0.018	0.003	1	18
N6/PPy10%/MMT	0.03	0.036	0.006	1	17
N6/PPy15%/MMT	0.045	0.054	0.009	1	16
N6/PPy20%/MMT	0.06	0.072	0.012	1	15
N6/PPy20%	0.06	0.072	0.012	–	16

sisting of N6 and PPy were prepared by the same method in the absence of MMT for comparison.

Characterization and electrical conductivity measurements

WAXD patterns were obtained by using a Simens D5000 diffractometer, with Cu Kα radiation (λ = 0.154178 nm) at 40 kV and 30 mA at a scanning rate of 0.04°/min.

The morphology of the synthesized composites was studied by SEM using an Oxford-Leo-440i SEM. DSC analysis were carried out on a Shimadzu DSC-60 DSC under air atmosphere at a heating rate of 5°C/min between 30 and 500°C.

TEM images were taken by using a PHILIPS CM-200 FEG TEM at 200-kV acceleration voltages. Samples were prepared by putting powdered nanocomposites into epoxy resin capsules, followed by curing the epoxy resin at 100°C for 24 h in a vacuum oven. Subsequently, the cured epoxy resin containing nanocomposites were cut with an ultramicrotome into 60- to 90-nm thick slices. The slices were then transferred on the surface of a 100-mesh copper grid for TEM observation.

A Perkin–Elmer Pyris Diamond TGA/DTA analyzer was used for TGA at a heating rate of 20°C/min between room temperature and 600°C under nitrogen atmosphere.

Electrical measurements were carried out on disk-shaped test samples prepared by compression-molding of the materials between two Ni foils by using a laboratory hot-press. The dimensions of the disks were 16 mm in diameter and 2 mm in overall thickness (each Ni foil was 0.1 mm in thickness). The process condition was 240°C mold temperature and 100 bar molding pressure. A copper wire was soldered on each Ni foil and electrical measurements were carried out after 24-h relaxation time. The variation of electrical resistivity with temperature was studied in a silicon oil bath with a temperature elevation rate of 3°C/min, and electrical resistivity was measured continuously by using a digital multimeter (Keader® LDM-852A) or LCR-meter (Escort® ELC-13C-131D). The measured electrical resistivities were converted into specific resistivity (ρ) by using simple geometric calculation: $\rho = R(A/L)$. In this equation, A was the test sample cross-section area and L, the sample thickness. Finally, the electrical conductivity (σ) obtained as reciprocal of ρ ($\sigma = 1/\rho$).

RESULTS AND DISCUSSION

Characterization of the ternary composites and the PPy/MMT nanocomposite

Figure 1 shows the SEM images for the original MMT and N6/PPy10%/MMT. Figure 1(b) shows the formation of PPy particles almost exclusively around the clay particles with bare N6 particles remaining uncovered. Therefore, there must be a tendency for PPy to accumulate around the clay particles, or pyrrole monomers adsorbed and then polymerized around the clay particles. On the other hand, WAXD results, which will be discussed later, have provided evidences for intercalation of PPy between the clay layers as well. The tendency toward clay particles may be due to the acidic characteristics of the clay, which attracts basic pyrrole monomers. Anionic characteristics of the clay layers also can be considered as another reason for attraction of postoxidized cationic PPy chains. Meanwhile, uncovered N6 particles provide an indication for absence of any interactions or compatibility between N6 and PPy. This may be due to their different molecular and polar characteristics.

As is mentioned in Characterization and Electrical Conductivity Measurements section, the composites were compression-molded at 240°C (i.e., above the
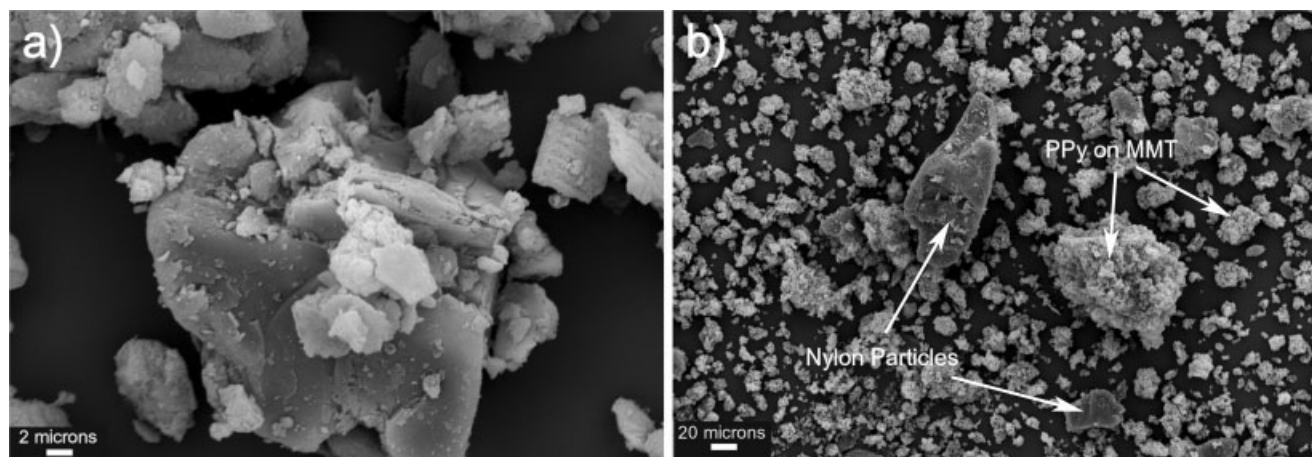

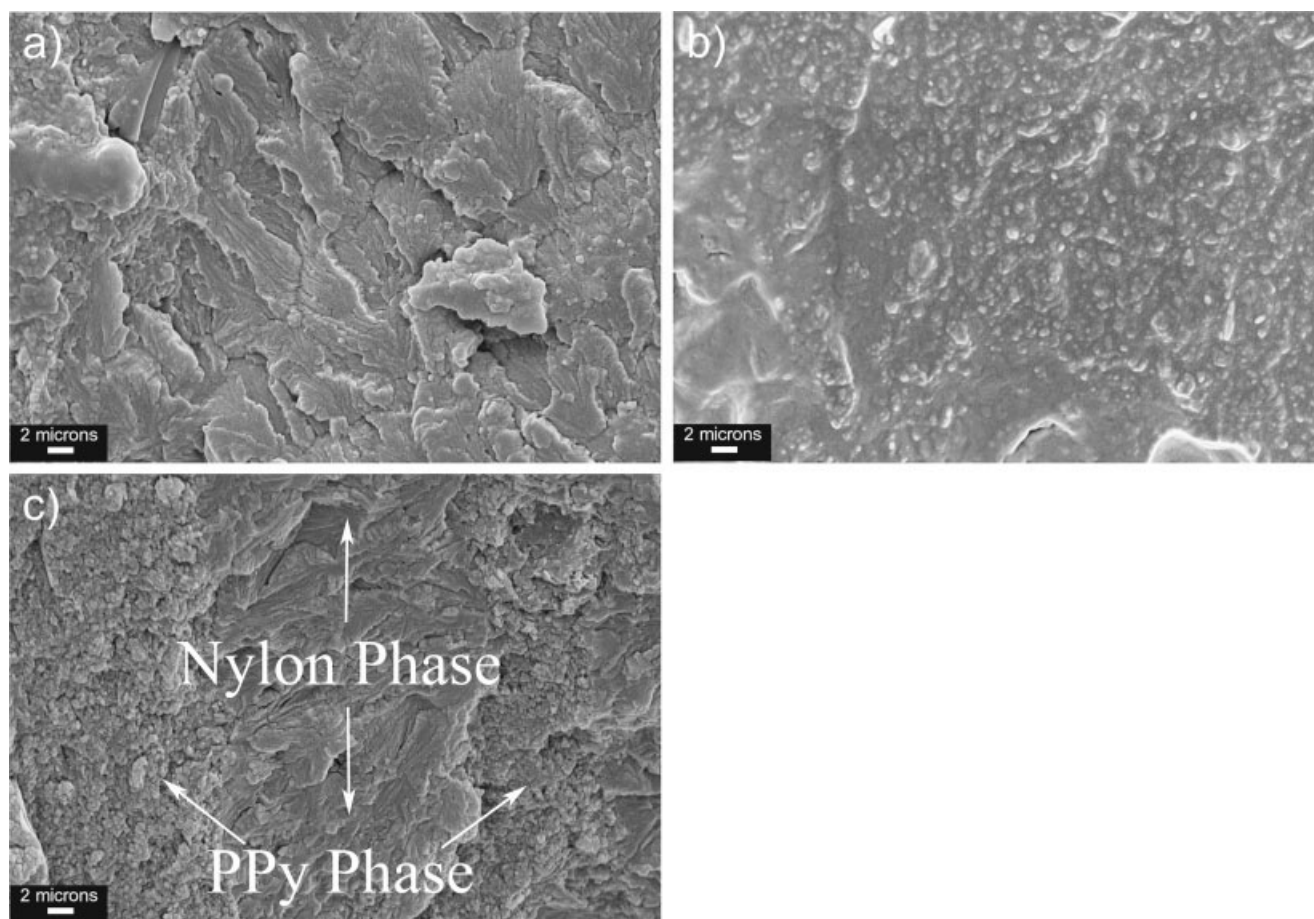**Figure 1** SEM micrograph for (a) original MMT and (b) N6/PPy10%/MMT.

Figure 2 SEM images form fracture surfaces of the molded compounds. (a) N6/PPy5%/MMT, (b) N6/PPy10%/MMT, and (c) N6/PPy15%/MMT.

melting point of N6), to prepare samples for electrical measurements. The morphology of the compounds after molding process was also studied by SEM. Figure 2 shows the results for fracture surfaces of the molded compounds: N6/PPy5%/MMT, N6/PPy10%/MMT, and N6/PPy15% /MMT. As is clear in Figure 2, the predominant phase is N6 when PPy content is low [Fig. 2(a), for example]. The lamellas of N6 can be seen all over the image in Figure 2(a) with PPy particles, which are resolvable as the minor phase around the image. However, PPy phase becomes more evident as its loading level increases in the composite. Finally, as PPy content increases in the composite, regions of PPy phase become detectable in the SEM micrographs, as is indicated in Figure 2(c) for the composite containing 15% PPy by weight. In this figure, N6 phase can be seen that is surrounded by two PPy regions. Although the two-phase structure exists in all the images in Figure 2, however, the formation of individual PPy phase is resolvable in Figure 2(c) because of higher PPy content. The two-phase structure confirms the incompatibility of N6 and PPy, as discussed earlier in previous paragraph.

Figure 3 shows the X-ray diffraction (XRD) patterns for MMT [Fig. 3(a)], N6/PPy10%/MMT [Fig. 3(b,b')], N6/PPy20%/MMT [Fig. 3(c,c')], and PPy/MMT [Fig. 3(d)]. The inset in Figure 3 shows the diffraction pattern up to 10° two-theta. The broad peak appearing at 5.8 (2θ scale) for the original MMT in Figure 3(a) is the diffraction peak from (001) planes of the layered silicate, which is equal to 1.5-nm basal spacing according to Bragg's law. As can be seen, the peak is shifted toward lower 2θ angles in Figure 3(b',c') for the composites and in Figure 3(d) for PPy/MMT nanocomposite. The reason for the observation of two intercalation peaks is not clear. However, in our previous work[20] in which PPy/MMT nanocomposites were prepared by several methods, the XRD studies showed that the diffraction pattern in PPy/MMT nanocomposites is dependent on the method of preparation, extensively to the oxidizing agent $Fe_2(SO_4)_3$ or $FeCl_3$ used. The overall result from the XRD studies is that intercalation occurs by PPy chains inside the gallery spacing of the MMT layers. TEM images, which are shown in Figure 4 for PPy/MMT, show the layers of MMT that are intercalated by PPy chains. Therefore, the ternary
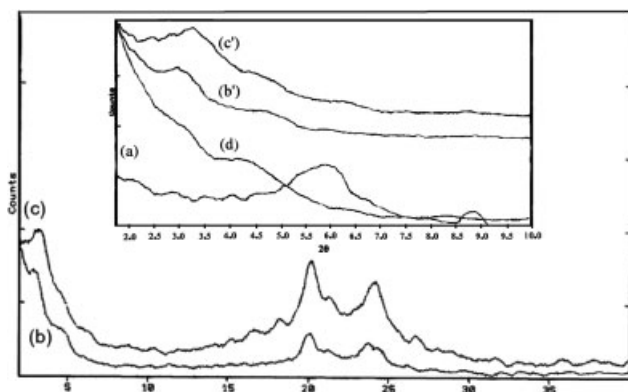
Figure 3 WAXD patterns for original MMT (a), N6/PPy10%/MMT (b and b'), and N6/PPy20%/MMT (c and c').

composites prepared in this work are composites of the intercalated PPy/MMT nanocomposites inside N6 matrix. Another result from Figure 3 is the change in N6 crystalline structure. N6 diffraction peaks appeared between 20 and 25 two-theta degrees in Figure 3(b,c). Peaks centered at 20° and 24.5° is the diffraction peaks from α crystalline form of N6, while the peak at 21.5 two-theta arise from the γ form. Comparison of Figure 3(b,c) reveals the increasing of the γ form by increasing PPy loading level in the composite. The change in crystalline structure has been reported for N6/MMT nanocomposites.[10] However, in the composite series being discussed here, formation of N6/MMT nanocomposite is not conceivable, and therefore, the change in crystalline form can be attributed to the effect of PPy/MMT content in the composite. The change in crystalline structure of N6 was confirmed also by DSC results, which will be discussed later in the following sections.

Electrical conductivity properties

Although electrical conductivity in conductive polymeric systems is measured usually by the four-probe method, however, we measured electrical conductivity of the composites by using a different method. We used disk-shaped test samples described in Preparation of the Reference Materials section for the electrical measurements. The method is usually used for the electrical measurements of the polymeric materials filled with conductive fillers.[21] The possibility of using common electrical measurement tools such as an ohm-meter, ease of preparation of the test samples, and facile investigation of the conductivity–temperature behavior is among the advantages of the method. Moreover, in this method, the materials reflect functionality, as they will do in true service condition in an electrical or electronic circuit for example. On the other hand, four-probe method

measures the surface conductivity while bulk conductivity can be measured by the mentioned method. However, it is worthy to note that the preparation of the test samples by the compression-molding can be done only if the materials are processable.

Table II summarizes the room temperature electrical properties measured for N6/PPy/MMT composites. Data in Table II, as is depicted in Figure 5, show the electrical conductivity increasing with increasing PPy content in the composites. A conductivity threshold was observed around 15% PPy loading by weight. Discussion provided in Characterization of the Ternary Composites and the PPy/MMT Nanocomposite section and the results from SEM studies showed that PPy and N6 are not compatible polymers at all and they form a two-phase structure in the molded compounds. At low PPy content, the PPy phase remains only in separate state in discrete regions inside the N6 matrix. However, PPy forms a connected network when its content reaches to amounts higher than that of the conductivity thresh-
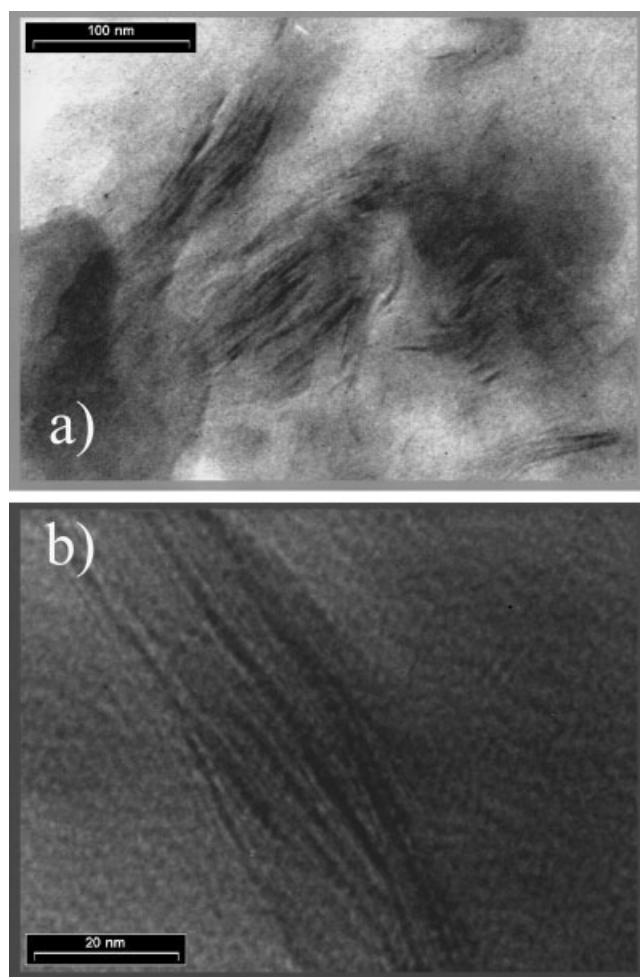

Figure 4 TEM images of PPy/MMT showing the intercalated clay layers by PPy (a) by lower and (b) by higher magnification.

TABLE II
Electrical Properties of N6/PPy/MMT Nanocomposites at Room Temperature

Nanocomposite	Electrical resistivity, R (kΩ)	Volume specific resistivity, ρ (Ω cm)	Electrical conductivity, σ (S/cm)
N6/ PPy5%/MMT	284.8	2.29×10^6	4.37×10^{-7}
N6/PPy10%/MMT	135.6	1.10×10^6	9.07×10^{-7}
N6/PPy15%/MMT	18.92	1.49×10^5	6.71×10^{-6}
N6/PPy20%/MMT	0.7526	6.01×10^3	1.66×10^{-4}

old. Therefore, in this case, PPy chain interactions inside the continuous network fulfill the requirements for the bulk conductivity of the whole composite. The conductivity threshold is therefore the borderline for the formation of the continuous network, which is dependent to the PPy loading level. This is in contrast to the tunneling conduction theory provided for the filled polymeric systems, such as polymer/carbon black composites, which exclude the necessity of physical contact between the conducting fillers. However, this is in agreement with the conduction theory proposed for the electrically conductive polymers, which assumes the necessity of interchain interactions for bulk conductivity.[13]

A conductivity threshold also has been observed and reported for several types of PPy/polymer composites measured by four-probe method. however, in lower amounts around 10–12% by weight of PPy.[1,8]

Interesting results were obtained from electrical resistivity–temperature property investigations. Figure 6 shows the result for N6/PPy5%/MMT. As can be seen, the electrical resistivity increases gradually with temperature below 100°C. This is absolutely in contrast with the electrical property observed for substantially conductive polymers including PPy. Conductivity increases or resistivity decreases with temperature in such systems because of thermally activated increased movements of the charge carriers in higher temperatures. However, the observed phenomena in our systems, i.e., gradually increasing of

resistivity with temperature looks like the commonly observed phenomena in polymers filled with conductive fillers.[21] This can be attributed to the thermal volume expansion of the matrix polymer, which results in more separation of the conductive fillers and, therefore, results in increased resistivity. This may also be attributed to the specific method of the electrical property measurements, which uses two metallic electrodes in both sides of the conductive composite and is different with the four-probe method usually used for substantially conductive polymeric systems. In Figure 6, after the initial and slow increase in resistivity, the resistivity starts to increase dramatically at specific temperature (T_{max}), reaches to a maximum (ρ_{max}), and then decreases again with increasing temperature. The overall result is a resistivity peak in resistivity–temperature curve. The same behavior was observed for all other composites in this work. Table III shows the room temperature resistivity (ρ_{RT}), the resistivity at peak (ρ_{max}), ρ_{max}/ρ_{RT} ratio, and the peak temperature T_{max}. As can be seen, T_{max} appeared almost in the same temperature for all compounds listed in Table III around 100°C. The ratio of ρ_{max}/ρ_{RT} changes in a wide range of numerical values for different samples; however, its relatively high value shows a true resistivity increase at T_{max}.

Conductivity–temperature behavior has been investigated for several types of PPy and PPy composites in the literature.[1,8] However, there was not
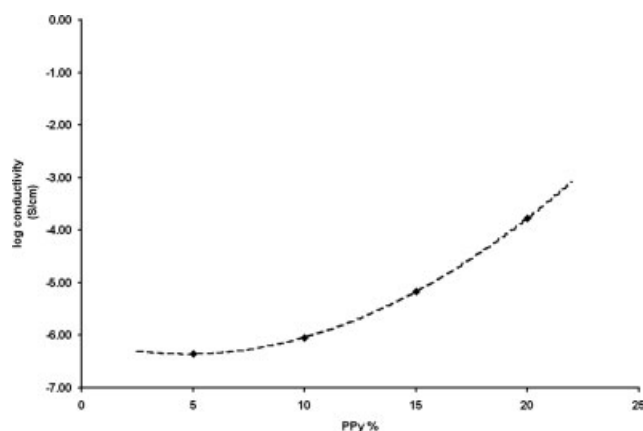

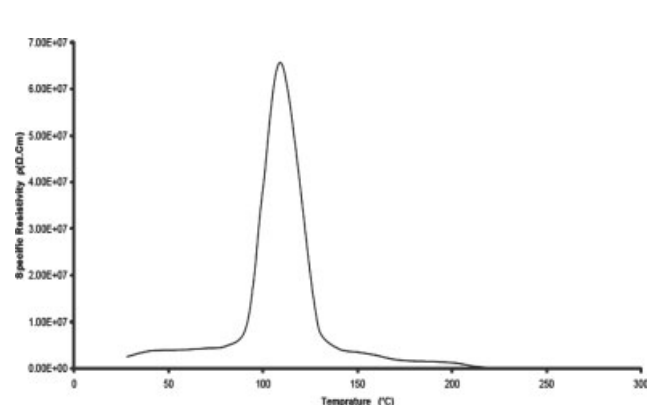Figure 5 Electrical conductivity variation with PPy content in N6/PPy/MMT nanocomposites.

Figure 6 Variation of electrical resistivity with temperature and the resistivity peak observed for N6/PPy5%/MMT nanocomposite.

TABLE III
Electrical Properties of Samples at Elevated Temperatures and Characteristics of the Resistivity Peak

Sample	Room temperature specific resistivity ρ_{RT}, (Ω cm)	Maximum specific resistivity ρ_{max}, (Ω cm)	ρ_{max}/ρ_{RT}	Temperature of the maximum specific resistivity, T_{max}
PPy	9.07×10^1	4.40×10^2	4.85	100
N6/PPy5%/MMT	2.55×10^6	6.53×10^7	25.61	110
N6/PPy10%/MMT	1.06×10^6	3.40×10^7	32.08	98
N6/PPy15%/MMT	1.85×10^5	1.53×10^6	8.27	100
N6/PPy20%/MMT	6.82×10^3	2.87×10^5	42.08	100
N6/PPy20%	3.07×10^3	1.43×10^4	4.66	110

any record available concerning to the resistivity peak observed in this work. In most cases, an Arrhenius type plot of conductivity–temperature or other mathematical models, such as variable range hopping,[22,23] has been considered to follow up the thermal activation energy of the conductivity increscent with temperature. Meanwhile, it has been reported that the conductivity–temperature behavior in PPy samples undergo a deviation from linearity around 100°C,[8] show a remarkable drop in conductivity from 75 to 100°C,[24] and different activation energies in both sides of 100°C, as computed from the Arrhenius model.[25]

Table III also contains the data for PPy and N6/PPy20% samples, which were synthesized according to the method described in Preparation of N6/PPy/MMT Composite of Nanocomposite section. Data shows the resistivity peak also for these two compounds and in the same T_{max} (100°C) again. Therefore, it can be concluded that the observed resistivity–temperature peak is due to PPy constituent in the ternary composites. On the other hand, the ρ_{max}/ρ_{RT} ratios in Table III increases with increasing PPy content in N6/PPy/MMT composites, except a big drop observed for N6/PPy15%/MMT, for which the reason is not clear.

To discuss about the observed temperature for the resistivity peak, a series of events can be considered to happen around 100°C for PPy and its composites. It has been investigated that the electrical conductivity increases with increasing water content in PPy composites.[26] Therefore, dehydration at 100°C might be considered as a reason for the observed resistivity peak, especially because PPy is a hygroscopic material. TGA was used to investigate the hypothesis. TGA curves are shown in Figure 7 for N6/PPy/MMT composites and compared with N6 and PPy. As can be seen, there is no significant weight loss around 100°C for none of the samples and only one principle decomposition peak exists for the compounds in Figure 7. Table IV summarizes the beginning decomposition temperature and char yield at 600°C. In Figure 7, TGA curves for N6/PPy/MMT composites follow almost the same pattern as compared to N6, except that the main decomposition

peak starts at lower temperatures as PPy content increases in the composite (Table IV). On the other hand, the residual weight at 600°C increases with increasing PPy content in the sample (MMT content is the same in all the composites). This is can be attributed to the thermal stability of PPy. Pure PPy starts to decompose at 300°C, in lower temperature than that of N6, however, it withstands higher temperatures so that it loses only 38% weight at 600°C.

In conclusion, the absence of dehydration around 100°C as studied by TGA suggests that dehydration does not exist and cannot be considered as the reason for the observed resistivity peak.

The other possible event around 100°C is the glass transition temperature, T_g, of PPy. This temperature has been reported to be at 103°C for pure PPy.[17] Figures 8 and 9 show the DSC curves for PPy and N6/PPy/MMT composites, respectively. A trace of T_g deflection on DSC curve can be resolved around 100°C for PPy in Figure 8 and in less extent in Figure 9 for the composites. DSC curves in Figure 9 also show the melting endotherm for N6 around 225°C. In addition to the sharp melting curve, which is due to melting of α-crystalline form of N6, a small shoulder is detectable at lower temperature side, which is attributed to the melting of γ-crystalline
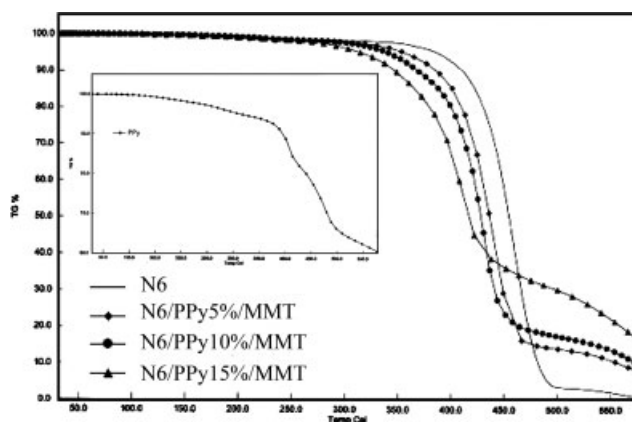

Figure 7 TGA curves for N6/PPy/MMT nanocomposites as compared with pure N6. The inset is TGA trace for pure PPy.

TABLE IV
Numerical Values for Thermal Properties of the Samples in Figure 7

Sample	Initial temperature for the main thermal decomposition peak (°C)	Char yield at 600°C (%)
PPy	300	63
N6	425	0
N6/PPy5%/MMT	405	8.75
N6/PPy10%/MMT	395	10
N6/PPy15%/MMT	370	16.25

Figure 9 DSC traces for N6 and N6/PPy/MMT nanocomposites under air atmosphere and 5°C/min heating rate.

form of N6. This provides a proof for the existence of both the crystalline forms α and γ, with the α-form as the predominant phase in the original N6. However, from Figure 9, the melting peak of α-form diminishes as PPy content increases in the composite. This confirms the previously discussed results obtained from WAXD studies about the effect of PPy on the crystallinity changes of N6.

The glass transition of PPy around 100°C and its correlation to the observed resistivity peak can be understood based on glass transition and conduction theories available. One of the widely accepted glass transition theories developed so far is the free expansion theory. Based on this theory, thermal expansion of free volumes, i.e., volumes not occupied by polymer chains, occurs below glass transition temperature. This is well described by Simha and Boyer model.[27]

$$v_f = v - (v_{0,R} + \alpha_G T)$$

In which v_f is the specific free volume, v the specific volume of the sample, $v_{0,R}$ specific volume of rubber at 0 K, α_G thermal volume expansion coefficient of glassy phase and T is temperature (K).

According to this model, specific free volume expansion occurs upon rising temperature below T_g. The expansion leads to more separation of interact-
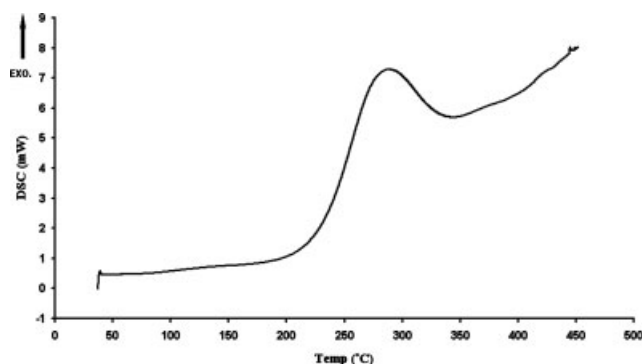
ing PPy chains and, therefore, to increasing the electrical resistivity with temperature. At temperatures above T_g, chains begin to fill the free volumes as a result of enhanced thermally motivated segmental motions of the chains in rubbery state. On the other hand, the mobility of the charge carriers also increases with temperature, so that it can be described by usual Arrhenius plot or other kinetic models.[1] The observed resistivity peak in resistivity–temperature curve suggests that around T_g the increased resistivity due to expansion of the free volumes dominates the normal and thermally induced decreased resistivity. At temperatures upper than T_g, the free volumes become filled with the rubbery chains and rebuilt interchain interactions lead to sharp decrease in resistivity followed by gradual decrease in resistivity with temperature.

CONCLUSION

N6, polypyrrole, and MMT composites of nanocomposite were prepared by using emulsion polymerization method in the presence of DBSNa as the surfactant. N6 provided the processability requirements for the composites, so that they were able to be compression-molded at N6 melting temperature. WAXD studies in addition to TEM images provided proofs for the formation of PPy/MMT-intercalated nanocomposites. Morphological studies carried out by SEM showed the formation and accumulation of PPy over MMT surfaces. Electrical measurement performed on the compression-molded samples showed a conductivity threshold for PPy content to be around 15% by weight. Two-phase structure consisting of separated N6 and PPy phases was detected for the molded samples. A peak was observed in resistivity–temperature investigations around 100°C for PPy, PPy/MMT nanocomposite, and the ternary N6/PPy/MMT composites. Studies carried out by

Figure 8 DSC curve for PPy under air atmosphere and 5°C/min heating rate.

TGA showed that dehydration cannot be the responsible factor for the observed resistivity peak. According to free volume expansion theory, the possible reason for the observed resistivity peak was discussed to be the glass–rubber transition of PPy.

References

1. Migahed, M. D.; Fahmy, T.; Ishra, M.; Barakat, A. Polymer Test 2004, 23, 361.
2. Omastova, M.; Chodak, I.; Pionteck, J. Synth Met 1999, 102, 1251.
3. Zhu, D.; Bin, Y.; Oishi, K.; Fukuda, Y. Macromol Symp 2004, 214, 197.
4. Kanatoma, T.; Tsuruta, A.; Tanaka, K.; Takeda, M.; Porter, R. S. Polym J 1983, 15, 327.
5. Kanamoto, T.; Ohama, T.; Tanaka, K.; Takeda, M.; Porter, R. S. Polymer 1987, 28, 1517.
6. Abbett, K. F.; Teja, A. S.; Kowalik, J.; Tolbert, L. J Appl Polym Sci 2003, 90, 1113.
7. Omastova, M.; Kosina, S.; Pionteck, J.; Jenke, A.; Pavlienc, J. Synth Met 1996, 81, 49.
8. Xie, H. Q.; Liu, C. M.; Guo, J. S. Polym Int 1999, 48, 1099.
9. Alexander, M.; Dubios, P. Mater Sci Eng 2000, 28, 1.
10. Ray, S. S.; Okamoto, M. Prog Polym Sci 2003, 28, 1539.
11. Oriakhi, C. O.; Lerner, M. M. Mater Res Bull 1995, 30, 723.
12. Hong, S. H.; Kim, B. H.; Joo, J.; Choi, H. J. Curr Appl Phys 2000, 1, 447.
13. Kim, J. W.; Liu, F.; Choi, H. J.; Hong, S. H.; Joo, J. Polymer 2003, 44, 289.
14. Liu, Y. C.; Ger, M. D. Chem Phys Lett 2002, 362, 491.
15. Liu, Y. C.; Tsai, C. J. Chem Mater 2003, 15, 320.
16. Yoshimoto, S.; Ohashi, F.; Kameyama, T. Macromol Rapid Commun 2005, 26, 461.
17. Yeh, J. M.; Chin, C. P.; Chang, S. J Appl Polym Sci 2003, 88, 3264.
18. Omastova, M.; Mravcakova, M.; Pionteck, J.; Haussler, L.; Chodak, I. Polym Eng Sci 2006, 46, 1169.
19. Mravcakova, M.; Omastova, M.; Potschke, P.; Pozsgay, A.; Pukanszky, B.; Pionteck, J. Polym Adv Technol 2006, 17, 715.
20. Peighambardoust, S. J.; Pourabbas, B. Macromol Symp 2007, 247, 99.
21. Pourabbas, B.; Peighambardoust, S. J. J Appl Polym Sci 2007, 105, 1031.
22. Kaynak, A. Turk J Chem 1998, 22, 81.
23. Roy, R.; Sen, S. K.; Digar, M.; Bhattacharaya, S. N. J Phys Condens Matter 1991, 3, 7849.
24. Gangopahya, R.; De, A. Eur Polym J 1999, 35, 1985.
25. Krishantha, D. M. M.; Rajapakse, R. M. G.; Tennakoon, D. T. B.; Dias, H. V. R. J Comp Mater 2006, 40, 1009.
26. Han, J. S.; Lee, J. Y.; Lee, D. S. Synth Met 2001, 124, 301.
27. Sperling, L. H. Introduction to Physical Polymer Science, 4th ed.; Wiley: New York, 2006.